University College Cork, Ireland
Coláiste na hOllscoile Corcaigh

Assessment of primary energy conversions of oscillating water columns. I. Hydrodynamic analysis

Wanan Sheng, Raymond Alcorn, and Anthony Lewis

Articles you may be interested in

Assessment of primary energy conversions of oscillating water columns. II. Power take-off and validations
J. Renewable Sustainable Energy **6**, 053114 (2014); 10.1063/1.4896851

Wave power calculations for a wave energy conversion device connected to a drogue
J. Renewable Sustainable Energy **6**, 013117 (2014); 10.1063/1.4862785

Performance of large arrays of point absorbing direct-driven wave energy converters
J. Appl. Phys. **114**, 204502 (2013); 10.1063/1.4833241

Dynamic response and stability of a flapping foil in a dense and viscous fluid
Phys. Fluids **25**, 104106 (2013); 10.1063/1.4825136

Erratum: "Quantitative time- and frequency-domain analysis of the two-pulse COSY revamped by asymmetic Z-gradient echo detection NMR experiment: Theoretical and experimental aspects, time-zero data truncation artifacts, and radiation damping" [J. Chem. Phys.129, 044505 (2008)]
J. Chem. Phys. **133**, 119902 (2010); 10.1063/1.3478222

Assessment of primary energy conversions of oscillating water columns. I. Hydrodynamic analysis

Wanan Sheng, Raymond Alcorn, and Anthony Lewis
Beaufort Research-Hydraulics and Maritime Research Centre, University College Cork, Cork, Ireland

This is an investigation on the development of a numerical assessment method for the hydrodynamic performance of an oscillating water column (OWC) wave energy converter. In the research work, a systematic study has been carried out on how the hydrodynamic problem can be solved and represented reliably, focusing on the phenomena of the interactions of the wave-structure and the wave-internal water surface. These phenomena are extensively examined numerically to show how the hydrodynamic parameters can be reliably obtained and used for the OWC performance assessment. In studying the dynamic system, a two-body system is used for the OWC wave energy converter. The first body is the device itself, and the second body is an imaginary "piston," which replaces part of the water at the internal water surface in the water column. One advantage of the two-body system for an OWC wave energy converter is its physical representations, and therefore, the relevant mathematical expressions and the numerical simulation can be straightforward. That is, the main hydrodynamic parameters can be assessed using the boundary element method of the potential flow in frequency domain, and the relevant parameters are transformed directly from frequency domain to time domain for the two-body system. However, as it is shown in the research, an appropriate representation of the "imaginary" piston is very important, especially when the relevant parameters have to be transformed from frequency-domain to time domain for a further analysis. The examples given in the research have shown that the correct parameters transformed from frequency domain to time domain can be a vital factor for a successful numerical simulation. © *2014 AIP Publishing LLC*. [http://dx.doi.org/10.1063/1.4896850]

I. INTRODUCTION

Oscillating water column (OWC) wave energy converters have been often regarded as the first generation of wave energy converters and maybe the most studied wave energy devices. The early success of oscillating water column wave energy converters saw that hundreds of small scale OWCs have been deployed to power the navigation buoys in remote areas (see Falcao[1] and Chozas[2]). The development has been since then advanced to large OWC wave energy plants and now some practical OWC plants have been built and actually generated electricity to the grid. It is reported that the LIMPET OWC plant has generated electricity to the grid for more than 60 000 h in a period of more than 10 years (Heath[3]). A recent development is the Mutriku OWC wave energy plant in Spain[4]—a multi-OWC wave energy plant with a rated power of 296 kW, consisting of 16 sets of "Wells turbines + electrical generator" (18.5 kW each), is estimated a electricity generation of 600 MW h so far. [EVE, Mutriku OWC Plant, http://www.fp7-marinet.eu/EVE-mutriku-owc-plant.html (accessed on 10/05/2014).]

OWC wave energy converters are one of the most adaptive concepts: they can be built on shoreline or breakwaters in a bottom-fixed fashion (LIMPET, PICO, and Mutriku OWC plants), or in near-shore in a form of either bottom-fixed or floating device or offshore in a form of floating devices. Its adaptivity may be only matched by the overtopping wave energy

6, 053113-1

converters, for example, the bottom-fixed Tapchan [Tapered Channel Wave Energy, http://taper-edchannelwaveenergy.weebly.com/how-does-it-work.html (accessed on 10/05/2014)] and the floating WaveDragon [Wave Dragon, http://www.wavedragon.net/index.php?option=com_frontpage&Itemid=1 (accessed on 10/05/2014)]. These types of the wave energy converters have a particular advantage over many other types of wave energy converters in the development stages: their pioneer wave energy plants can be simply built on shoreline. One advantage of the shoreline wave energy plants is that the problems with the wave-structure interaction (partially), cable connections, and access to the plant are not present (it is also noted that mooring system is not applied in this case), so that in their development stages, the focus can be more on the wave energy conversion and power take-off (PTO) (air turbine and control system and strategies). The experience accumulated and lessons learnt from these developments can be then easily transplanted to the floating OWC wave energy converters, in which the focus can be paid on the interaction of wave-structure, mooring system, and cabling connection since the issues with PTO and control system have been addressed in those pioneer plants.

The second advantage of the OWC wave energy converters is their unique feature in power conversion. In the OWC wave energy converters, the air flow is normally accelerated from the very slow airflow in the chamber (driven by the internal water surface (IWS)) to a high-speed airflow through the power take-off system by 50–150 times if the PTO air passage area ratio is taken 1:50–1:150 to the water column sectional area. This much accelerated air can drive the air turbine to rotate in a high speed, typically a few hundreds RPM for the impulse turbines and more than a thousand RPM for the Wells turbines (see O'Sullivan and Lewis[5]). The high-rotational speed of the air turbine PTO allows a direct connection to the generator, and thus the bulky gearbox may not be necessary, and more importantly, for a certain power take-off, the high rotational speed can also mean a small force or torque acting on the PTO system, which in turn ensures a high reliability in power take-off systems.

To understand and improve wave energy conversion by the OWC devices, numerical methods have been developed. Earlier theoretical work on the hydrodynamic performance of OWCs has shown that OWC devices could have a high primary wave energy conversion efficiency if the optimized damping can be attained (Sarmento and Falcao,[6] Evans,[7] and Evans and Porter[8]) for those fixed or simple OWC devices. For the more complicated and practical OWC devices, the boundary element method (BEM) (and the relevant commercial software, such as WAMIT [WAMIT, User Manual, www.wamit.com/manual.htm (accessed on: 10/05/2014)], ANSYS AQWA [AQWA User Manual, www.mecheng.osu.edu/documentation/Fluent14.5/145/wb_aqwa.pdf (accessed on 10/05/2014)], etc.) can be readily available for any complexity of the geometries. Regarding the full scale device, there may be air compressibility problems. Due to the nonlinearity and the non-Froude similarity nature (see Weber[9] and Sheng et al.[10]), the air compressibility in the air chamber may not be evident or present in the small scaled models because the scaled models have normally small scaled air volumes and pressures in the air chamber. Sarmento et al.[11] have proposed a linearized formula for the flowrate through the power take-off system, based on an assumption of an isentropic flow. Sheng et al.[12] have recently formulated a full thermodynamic equation for the air flow in the chamber by invoking the simple PTO relation of the chamber pressure-flowrate which, though simple, has included all the effects of the flow through the air turbine, hence, the detailed complicated air flow through the turbine can be avoided (note: for improving the performance of the air turbine, the detailed air flow through the turbine is still very important if the turbine performance is examined). More recently, Sheng et al.[13] have also coupled the hydrodynamics and the thermodynamics for a bottom-fixed generic OWC device and have predicted the internal water surface and chamber pressure very well when compared to the experimental data.

So far, though successful to some extent, a reliable numerical simulation for the performance of the OWC wave energy converters is not available yet. Hence, the development of OWC wave energy converters frequently relies on the experiments in laboratories. Essentially, physical models include all the effects if the scaling is well prepared. For instance, the model should be large enough to ensure the scaling correct in which the Reynolds number would be large enough to minimise the Reynolds effect (see Sheng et al.[10]). In physical model tests, the scaled OWC models mean smaller air chambers and smaller chamber pressure responses, and

therefore, the air compressibility (i.e., the "spring-like effect") cannot be scaled and present. Nonetheless, experiments could provide valuable assessments to the performance of the OWC devices if the model tests are well conducted. For example, experimental studies on the bottom-fixed or floating OWCs have shown that the wave energy conversion efficiency of an OWC device very much depends on the damping coefficients of the flow passing through the power take-off system, as well as the size and length of the water column (water column sectional area and length). Toyota *et al.*[14] have shown that both the size of the air chamber and the length of the horizontal duct length of a Backward Bent Duct Buoy (BBDB) device have significant effects on the primary power conversion of the OWC wave energy converters. Imai *et al.*[15] have studied the influence of the horizontal duct length to the wave energy capture capacity in a BBDB device and shown that a longer horizontal duct has increased the maximum IWS response to a longer resonance period. As a result of this, a longer horizontal duct may be desirable for tuning the BBDB to the wave states of longer wave periods. Morris-Thomas *et al.*[16] have experimentally studied the hydrodynamic efficiency on fixed OWCs with different front shapes. From the comparison, it can be seen that the front shapes have some but limited influence on the wave energy conversion efficiencies of the fixed OWC. For the four different front shapes, the wave energy capture efficiencies are overall similar, and the maximum wave energy conversion efficiency is about 70%, but no reason has been given why the maximum wave energy conversion efficiency is only about 70%.

Generally, reliable numerical assessments have not been well established for OWC wave energy converters though this type of wave energy converter has been widely studied and may have a longest history when compared to other types of wave energy converters. In this research, the focus is on the development of a numerical assessment method for the hydrodynamic performance of OWC wave energy converters, and the details on how to reliably assess the hydrodynamic performance, which is a prerequisite condition in the overall performance assessment for an oscillating water column wave energy converter, are presented and discussed. Examples have shown that special care must be taken if a reliable hydrodynamic model is deemed to be developed for the OWC wave energy converter.

II. METHODOLOGY

A. Frequency domain analysis

Potential theory has been well-developed in the last century and now widely used in marine and offshore applications, and more recently applied in wave energy conversions, including the oscillating water column devices.

For some specific OWC devices, such as two-dimensional OWC devices, or some three-dimensional OWCs with simple structures, analytical solutions are possible (Evans and Porter,[8] Martins-rivas and Mei,[17] and Mavrakos and Konispoliatis[18]), but more popular approaches are the numerical analysis using the commercial codes based on the boundary element method, such as WAMIT and ANSYS AQWA. These commercial codes are readily available for any geometry of interest.

Based on the assumption of the potential flow, the velocity potential of the flow around the floating structure satisfies the Laplace equation,

$$\nabla^2 \varphi = 0, \tag{1}$$

where φ is the frequency-domain velocity potential of the flow around the floating structure (the corresponding time-dependent velocity potential should read $\Phi = \varphi e^{i\omega t}$ since the dynamic system is assumed to be linear in the hydrodynamic study).

An earth-fixed coordinate system is defined for the potential flow problem. The coordinate is fixed in such a way that the x-y plane is on the calm water surface and z-axis positive up vertically. In the coordinate, the free surface conditions can be expressed in the frequency domain (see Lee and Nielsen[19]), as

$$\frac{\partial \varphi}{\partial z} - \frac{\omega^2}{g} \varphi = \begin{cases} 0, & (on \; S_f) \\ -\dfrac{i\omega}{\rho g} p_0, & (on \; S_i), \end{cases} \qquad (2)$$

where ω is the wave frequency, ρ is the density of water, g is the acceleration of gravity, p_0 is the pressure amplitude acting on the internal free surface, S_i is the internal free surface in the water column, and S_f is the free surface but excludes the internal free surface.

It must be noted that the pressure amplitude acting on the internal free surface is an unknown, which must be solved when a power take-off system is applied.

Hydrodynamically, the water surface in an OWC can be regarded as a moonpool, which has been found applications in the operations of offshore platforms and studied in theoretical and numerical approaches (see Refs. [20–23]). The difference between a moonpool and an oscillating water column is that the application of the power take-off system in the OWC wave energy converters will apply a reciprocating pressure (the alternative positive and negative chamber pressure, and they may be nonlinear if the nonlinear PTO is applied) on the internal water surface, which would make the problem more complicated.

To solve the linear hydrodynamic problems in the OWC wave energy devices, different approaches have been developed and used. The popular approaches include the massless piston model[19,24] and the pressure distribution model.[7] In the former approach, the internal free surface is assumed to behave as a massless rigid piston (a zero-thickness structure), and the target solution is the motion of the internal water surface. The internal water surface motion is then coupled with the PTO so that the chamber pressure can be solved. A slightly different version of the massless piston model is a two-body system for the OWCs, in which the first rigid body is the device itself and the second rigid body is an imaginary thin piston at the internal free surface to replace part of the water body in the water column. Hydrodynamically, the two-bodies are strongly coupled (see Refs. [13], [25], and [26]). By applying a power take-off system, the relative motion between the two-body could produce a reciprocating pressure in the air chamber. In the latter approach, the internal free-surface condition is represented in terms of the dynamic air pressure in the chamber (see Refs. [27] and [28]) and in the numerical simulation, a reciprocity relation must be employed as shown by Falnes[29] so that the conventional BEM can be used. However, it must be pointed out that this method may be only applicable for the cases of linear PTOs. Tank test and field test data have shown the nonlinear chamber pressure (with both wave frequency and high frequency components in regular waves) even though the internal water surface motion can be reasonably linear when a nonlinear PTO is applied for wave energy conversion.

Relatively, the physical meaning of the first approach is more obvious, and its implementation in the numerical assessment is more straightforward. Hence in this research, this approach is applied and studied.

To represent the dynamic system better, a convention for a two-body system is used: The motion modes of the first body are given by x_i ($i = 1, 2,\ldots, 6$), corresponding to the first rigid body motions of surge, sway, heave, roll, pitch, and yaw, respectively, and the motion modes of the second body are given as x_i ($i = 7, 8,\ldots, 12$), which corresponds to the 6 degrees of freedom motion of the second body, i.e., surge, sway, heave, roll, pitch, and yaw. To simplify the analysis in the oscillating water column wave energy conversion, only the heave motions of the two bodies are considered for power conversion, because for power conversion in the OWC, the other motion modes may not be useful in contributing to generate power in this particular case, and because it is generally acceptable when the motions are not too severe, the heave motions may not be coupled with other types of motions (the generic OWC considered in the research has an axi-symmetrical structure).

The heave motions of the two bodies in frequency domain can be written as

$$\begin{cases} \{-\omega^2[m_{33} + a_{33}(\omega)] + i\omega b_{33}(\omega) + c_{33}\}\zeta_3 + \{-\omega^2 a_{39}(\omega) + i\omega b_{39}(\omega) + c_{39}\}\zeta_9 = f_3(\omega), \\ \{-\omega^2 a_{93}(\omega) + i\omega b_{93}(\omega) + c_{93}\}\zeta_3 + \{-\omega^2[m_{99} + a_{99}(\omega)] + i\omega b_{99}(\omega) + c_{99}\}\zeta_9 = f_9(\omega), \end{cases} \qquad (3)$$

where m_{33} and m_{99} are the masses of the first and the second bodies; $a_{33}(\omega)$, $a_{39}(\omega)$, $a_{93}(\omega)$, and $a_{99}(\omega)$ are the frequency-dependent added masses for the heave motion for the first and second bodies and their interactions at the infinite frequency; c_{33}, c_{99} and c_{93}, c_{39} are the restoring force coefficients and their interactions (hydrostatic coefficients); b_{33}, b_{99} and b_{93}, b_{39} are the hydrodynamic damping coefficients for heave motions and their interactions; f_3 and f_9 are the excitations for the first and second bodies, and ζ_3 and ζ_9 are the complex heave motion amplitude of the two bodies, respectively.

Solving Eq. (3), the relative heave motion (complex) between the two bodies termed as the IWS can be calculated as

$$\zeta_r = \zeta_9 - \zeta_3. \tag{4}$$

Here, ζ_3 and ζ_9 are the complex heave motion amplitudes for both bodies.

Accordingly, the amplitude responses of the device heave motion, X_3, the piston heave motion, X_9, and the internal water surface motion, X_r, are given as follows:

$$\begin{cases} X_3 = \dfrac{|\zeta_3|}{A} \\ X_9 = \dfrac{|\zeta_9|}{A}, \\ X_r = \dfrac{|\zeta_r|}{A} \end{cases} \tag{5}$$

or

$$\begin{cases} X_3 = \dfrac{2|\zeta_3|}{H} \\ X_9 = \dfrac{2|\zeta_9|}{H}, \\ X_r = \dfrac{2|\zeta_r|}{H} \end{cases} \tag{6}$$

where A and H are the amplitude and height of the incoming wave, respectively, and $|*|$ means the modulus of the complex response.

B. Time domain analysis

For OWC wave energy converters, the whole dynamics may very likely be nonlinear if an air turbine PTO take-off system is included, for example, a linear Wells turbine. When a full scale OWC device is considered, the air chamber and the pressure can be large enough, so that the air compressibility in the air chamber can be obvious (see Falcao and Justino[30]), which is essentially nonlinear. If mooring system is included, the nonlinearity will be more obvious when the large motions of the device are induced. For a nonlinear dynamic system, frequency-domain analysis is no longer suitable; hence a time domain analysis must be employed.

In the time-domain analysis in the research work, the Cummins-Ogilvie hybrid frequency-time domain analysis is used, in which the hydrodynamic parameters can be first analysed in frequency domain, and then the Cummins time-domain equation is established using the Ogilvie's relation (Cummins[31] and Ogilvie[32]). This hybrid frequency-time domain approach has been a popular choice in the development of wave energy conversions.[27,33–36] The nonlinear effects from PTO or any other sources can be fully implemented in the time-domain analysis.

1. Time domain equations

To simplify the problem in the oscillating water column wave energy conversion, we assume only the heave motions of the two bodies are useful for power conversion. The

assumption may be acceptable when the motions are not too severe, and the heave motion may not be coupled with other types of motions, especially for the cylinder-type structures.

The heave motion of the two bodies can be written in time-domain as

$$[m_{33} + A_{33}(\infty)]\ddot{x}_3(t) + \int_0^t K_{33}(t-\tau)\dot{x}_3(\tau)d\tau + C_{33}x_3(t) + A_{39}(\infty)\ddot{x}_9(t)$$
$$+ \int_0^t K_{39}(t-\tau)\dot{x}_9(\tau)d\tau + C_{39}x_9(t) = F_3(t), \tag{7}$$

$$A_{93}(\infty)\ddot{x}_3(t) + \int_0^t K_{93}(t-\tau)\dot{x}_3(\tau)d\tau + C_{93}x_3(t) + [m_{99} + A_{99}(\infty)]\ddot{x}_9(t)$$
$$+ \int_0^t K_{99}(t-\tau)\dot{x}_9(\tau)d\tau + C_{99}x_9(t) = F_9(t), \tag{8}$$

where m_{33} and m_{99} are the masses of the first and the second bodies; $A_{33}(\infty)$, $A_{39}(\infty)$, $A_{93}(\infty)$, and $A_{99}(\infty)$ are the added masses for the heave motion for the first and second bodies and their interactions at the infinite frequency; C_{33}, C_{99} and C_{93}, C_{39} are the restoring force coefficients and their interactions; K_{33}, K_{99} and K_{93}, K_{39} are the impulse functions for heave motions and their interactions; F_3 and F_9 are the excitations for the first and second bodies.

The impulse functions can be obtained if the frequency-domain added mass or damping coefficients have been assessed via the transform as

$$K_{ij}(t) = \frac{2}{\pi}\int_0^\infty b_{ij}(\omega)\cos\omega t d\omega, \tag{9}$$

or

$$K_{ij}(t) = \frac{2}{\pi}\int_0^\infty \omega[a_{ij}(\omega) - a_{ij}(\infty)]\sin\omega t d\omega, \tag{10}$$

where a_{ij} and b_{ij} are the added mass and damping coefficients in frequency domain, $a_{ij}(\infty)$ is the added mass at the infinite frequency, which is a frequency-independent value.

2. IWS motion in time domain

The internal water surface in the water column is the parameter for creating a reciprocating chamber pressure in the air chamber, thus the pneumatic power which can be used for power conversion. The internal water surface motion is given by the relative heave motions of the two bodies as

$$x_r(t) = x_9(t) - x_3(t). \tag{11}$$

III. PISTON REPRESENTATION

To illustrate the problem more clearly, a cylindrical OWC wave energy converter is considered here. This is a generic OWC wave energy converter which has been widely tested and studied in HMRC wave basin (see Sheng et al.[37]). A photo of the device is shown in Figure 1.

The OWC device has a schematic drawing of the vertical section shown in Figure 2. The whole column of the device (the water and air columns) has a diameter of 0.23 m, and an overall length of 0.3 m, of which 0.15 m is emerged in water (i.e., a draft of 0.15 m). The device has a float of 0.04 m thick and 0.2 m high surround the entire column providing the buoyancy and stability for the device and 0.10 m submerged in water. A circular plate is fixed on the top

FIG. 1. A generic cylinder OWC wave energy converter.

of the air column, with an orifice in middle to model a nonlinear PTO take-off (that is, a non-linear air turbine PTO). The overall weight of the device is 3.39 kg. The device was also ballasted for a good stability to float rightly in the waves.

As shown in Figure 2, a piston is used to represent part of the water body in the water column (in the figure half of the length of the water body in the device column), whose motion can be equivalent to the uniform motion of the water body in the water column. For wave energy conversion, the up-and-down motions of the piston relative to the column structure can generate a pressurised and de-pressurised air in the air chamber which could exhale or inhale air through the air turbine and to drive it to rotate, so to generate electricity if it is connected to a generator.

A. Natural period of the piston motion

As shown by Evans and Porter,[8] the interior free surface has a natural period, T_0, if the length of the cylinder is much larger than its diameter (actually this condition is not well satisfied in this case, but for a comparison, the formula is used) as
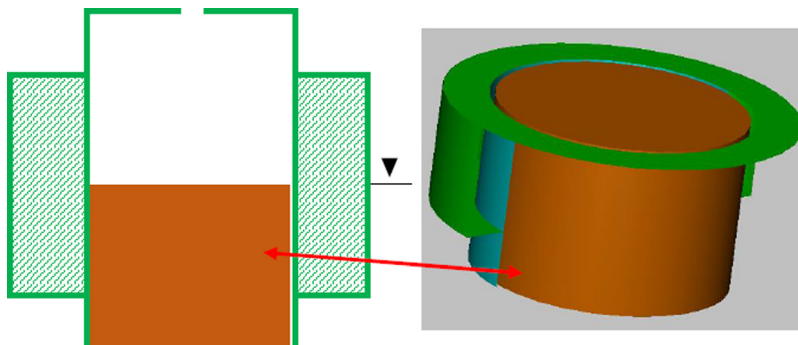

FIG. 2. Water column in water and the corresponding piston (the length of the piston is same as the full length of the water column).

$$T_0 = 2\pi\sqrt{\frac{D}{g}} = 0.777s, \tag{12}$$

where D (=0.15 m) is the draft of the water depth or the length of the water column and g the gravity acceleration. This formula corresponds to the natural period of a cylinder of a draft D in water without a correction from the added mass.

If the imaginary piston is considered as an isolated cylinder, its added mass for the heave motion has been given according to McCormick (Ref. 38, p. 48) when the draft D is far larger than its diameter (again, this condition is not fully satisfied. But unlike the previous case, the added mass has been included. And for comparison, the formula is again used here) as follows:

$$a_{33} = 2.664\rho R^3, \tag{13}$$

where R is the radius of the cylinder.

The corresponding natural period of the heave motion would be

$$T_0 = 2\pi\sqrt{\frac{D + 0.848R}{g}} = 0.998s. \tag{14}$$

For a large water column or a moonpool, its natural period of the water surface motion has been studied by Veer and Thorlen,[23] and they gave a formula for the calculation of the natural period of the internal water surface motion as

$$T_0 = 2\pi\sqrt{\frac{D + 0.41 * S_0^{1/2}}{g}} = 0.970s, \tag{15}$$

where S_0 is the sectional area of the moonpool/water column.

A more appropriate approach in obtaining the internal water surface motion, and thus its relevant natural period is employing the conventional BEM (in this case, WAMIT). In the BEM code, the interaction between the water body and the floating structure is fully accounted. Hence, the natural period of the internal water surface would be more accurately calculated via the BEM.

All the natural periods using different formulas, including the one obtained from WAMIT simulation are listed in Table I. One can see that those semi-empirical and numerical methods give quite similar estimations to the natural period of the internal water surface motion if an appropriate added mass can be included.

In this study, WAMIT has also been used to study the behaviour of the device and the internal water surface. In the simulation, the two-body system has been used. Figure 3 shows that the device and the piston have different natural periods (two spikes in the responses in Figure 3), that is, the imaginary piston has a natural period of 0.935 s, which is close to the results from Eqs. (14) and (15), but larger than that given by Eq. (12), whilst the heave motion of the device has a natural period of 0.740 s.

From Figure 3, it can be also seen that both heave motion responses of the device and the piston are modified due to their interaction. For the heave response of the device, there is a

TABLE I. Natural periods of the internal water surface.

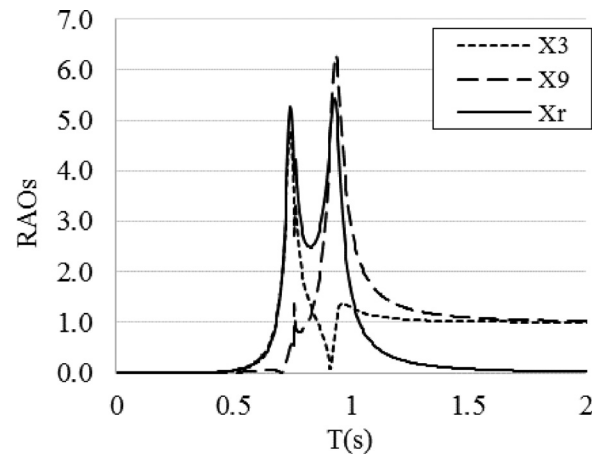| Method	Natural period of internal water surface, T_0	Reference
Evans *et al.*	0.777 s	8
McCormick	0.998 s	38
Veer *et al.*	0.970 s	23
WAMIT	0.935 s	…

FIG. 3. Responses of the heave motions of the float and the piston and their relative motion (X3-heave response of the device; X9-heave response of the piston; Xr-the relative response of the internal water surface).

small response when the wave period is at the natural period of the piston heave motion; while for the piston response, due to the heave motion of the device, the response is modified significantly when the wave period is at the natural period of the heave motion of the device. As a result of the relative heave motion between the cylinder and the piston, the IWS motion (Xr) has two peaks which correspond to the natural periods of the device and the piston heave motion, respectively. All three responses have large peak values (more than 5.0). This is mainly because in WAMIT, only hydrodynamic damping is considered, while the other types of the damping, for instance, the viscous damping, are ignored in the analysis.

B. Piston length and motion responses

As it is well known that, in many cases in studying an OWC wave energy converter, the water column of an OWC device has been represented by a thin piston or a zero thickness structure.[25,26] The zero thickness structure is replaced the internal free surface (see Figure 4). It has been shown theoretically by Falcao et al.[25] (also Evan et al.[24]) that the added mass for the thin rigid-body is the entire entrained-water by the water column plus some additional added-mass. This interesting result can be taken that the mass of the thin piston plus the entrained water (i.e., the major part of the corresponding added-mass) may be possibly equivalent to that
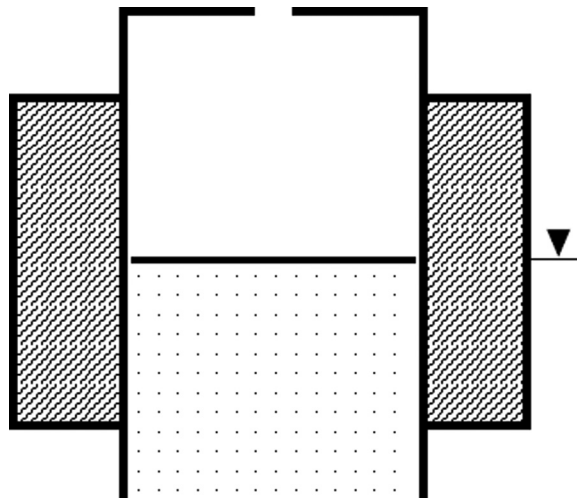

FIG. 4. A very thin piston on the internal free surface (L is small or zero).

of a full piston. An extreme case of the thin piston is the zero thickness structure (i.e., a massless piston), which has been also studied by Lee *et al.*[19,39] via a method called "generalised modes," and the generalised modes for the internal water surface motion can be simply specified as the additional motion modes in the boundary element codes, so that a significant modification to the code is not necessary. As can be seen in many practical cases, the thin/massless pistons or the full pistons are both popular in studying the performance of an OWC device. Therefore, there may be a question, what will happen if a certain length of the piston is considered, as shown in Figure 5.

In the above OWC device, a longest piston length could be the full length of the water column of 0.15 m (i.e., $L = 0.15$ m, where L is the actual length of the piston), and the shortest piston length is zero in the massless piston (Figure 4). In-between, the length of the piston could be any length between 0.0 m and 0.15 m (Figure 5). In Figure 6, a comparison of the internal water surface responses for different piston lengths is shown (the lengths "$L = 0.001$ m," "$L = 0.01$ m," etc., indicating the lengths of the pistons). It can be seen that the IWS responses are very similar when the wave period is larger than 0.5 s for all five piston lengths (Figure 6). However, the values at the second peaks may be slightly different for the different lengths of the pistons, especially for the full length of the piston ($L = 0.15$ m). And in all these responses, there are two obvious resonances: the first resonance of a shorter period corresponds to the device heave motion resonance and the second resonance corresponds to the natural period of the pistons. From the comparison, it can also be seen that in the region of very short periods, the IWS responses can be very different for short pistons (see Figure 7): these response spikes may correspond to their inherent natural periods of the "pistons" when they are not isolated without the interaction from the water column structures. The shorter the piston, the shorter the natural period is (can be deduced from Eqs. (12), (14), or (15)). In the frequency domain analysis, the relative internal water surface motion responses are dominated by the heave responses of the two bodies. The small spikes of the motion responses in very short waves are often beyond any interest (not power extraction from that!).

It must be noted that in the IWS responses in Figures 6 and 7, they are only damped via their inherent hydrodynamic damping coefficients. Hence, the responses are relatively high at the corresponding resonance periods.

C. Piston length and added mass

When a time domain analysis is needed for the dynamics of the wave energy converter, the relevant hydrodynamic parameters can be obtained by a transform from frequency domain to time domain, based on the Cummins time domain equation[31] and the Ogilvie relation.[32] This
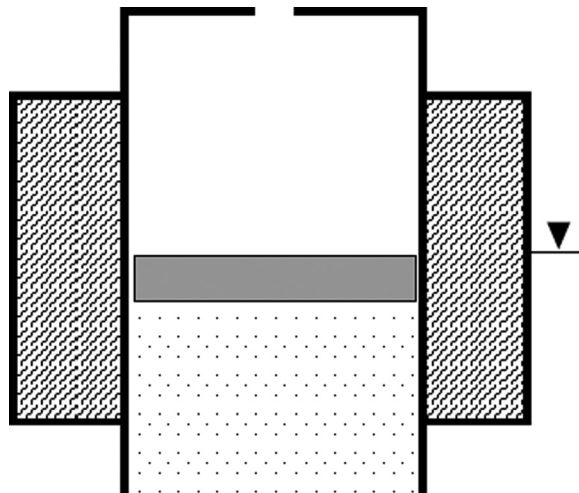

FIG. 5. An illustration of a thick piston for representing the internal free surface.
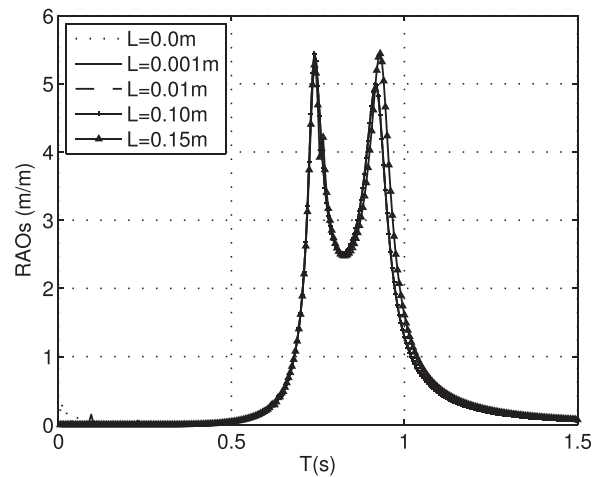
FIG. 6. IWS response predictions with a 2-body system.

method has been often named as hybrid frequency-time domain method[36] and very popular in the applications in wave energy conversion thanks to its low computation burden and its straightforward physical meaning. One important aspect in such an application is the assessment of the added mass at the infinite frequency, because this special added mass and the device mass itself can form the overall mass in the dynamic system in the time domain system, which in turn very much decides the dynamic responses of the system, especially the resonance response. Hence, its correctness is of vital importance in such a dynamic system.

Table II shows the masses and the added-masses at infinite frequency for the pistons and the device from the simulations using WAMIT. For the massless piston (its length $D = 0.0$ m), the "generalised modes" have been used, which represents the IWS motion (named as the mode 7), while for the cases of certain lengths of pistons, two-body system is used in WAMIT simulations.

From the table, the added masses for the device heave motion at the infinite frequency are very close except the one in the massless case, which is obviously "wrong" (a very large negative added mass!). And the added mass for the "generalised mode" is also wrong (even a larger negative added mass). For the cases of certain lengths of the pistons, the overall mass for the piston can be different, and their correctness will be examined later in this research. However, one can see that when the piston length is larger than 0.05 m, the overall mass (given by the mass and added mass together) is very similar, though the piston mass itself can be very different (2.08 kg for the piston length 0.05 m and 6.23 kg for the piston length of 0.15 m), see Figure 8.
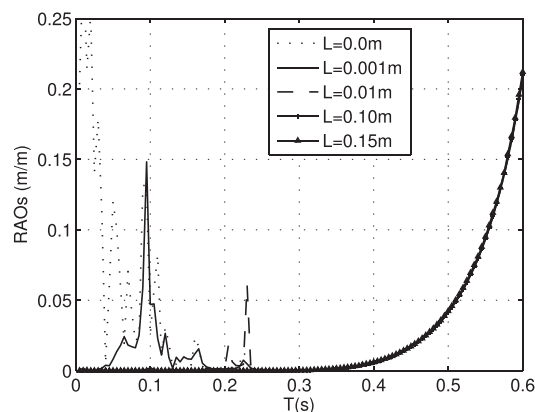

FIG. 7. IWS response predictions (zoom for the responses in short periods).

TABLE II. Piston mass and its added mass.

Piston L(m)	0	0.001	0.005	0.01	0.02	0.05	0.1	0.15
M_{33}	3.39	3.39	3.39	3.39	3.39	3.39	3.39	3.39
A_{33}	−43.44	1.43	1.44	1.44	1.45	1.45	1.45	1.46
$A_{77}(\infty)$	−70.10	…	…	…	…	…	…	…
M_{99}	…	0.04	0.21	0.42	0.83	2.08	4.15	6.23
$A_{99}(\infty)$	…	4.35	5.77	6.30	6.66	6.43	4.66	2.93
$M_{99}+A_{99}(\infty)$	…	4.39	5.98	6.72	7.49	8.51	8.81	9.16

Figure 9 shows a comparison of the added mass for four different lengths of the pistons. From the figure, it can be seen that for the cases of small lengths of the piston, its added mass can be a large positive or negative value at certain short periods. These very spiky added masses (both large positive and negative) happen at the different periods for the different lengths of the pistons ($T = 0.76$ s for $L = 0.15$ m, $T = 0.445$ s for $L = 0.05$ m, and so on), the corresponding periods should be very close to the piston natural periods in the absence of the interaction between the piston and the device. Figure 10 shows a comparison for long ($L = 0.10$ m and $L = 0.15$ m). For the cases of piston lengths of 0.10 m and 0.15 m, the added mass may still be spiky at very short waves, where the negative and positive added masses can be seen clearly, but not as severe as those of shorter pistons.

The added mass in high frequencies (very short waves) are difficult to calculate, though in WAMIT, it is possible to specify a simulation so that the added mass at infinite frequency can be calculated. However, in many practical cases, we may assume that the added mass at a frequency large enough can be taken as the added mass at infinite frequency. Then a question may arise: how large of the frequency is enough?

Figure 11 shows the added mass calculations in very short waves of wave periods from 0.005 s to 0.25 s, which correspond to high frequencies 25.1 rad/s and 1256 rad/s, respectively, for the pistons with different lengths. It can be seen that the added mass for $L = 0.15$ m and $L = 0.05$ m are very steady in most of the periods, but not in the very short wave periods. For the case of $L = 0.001$ m, the added mass tends to be steady, but it is very close to zero. Obviously, it is not correct, and the issue will be further discussed later in this research. For the case of the piston $L = 0.01$ m, it is varying very much at all high frequencies.

To calculate the internal water surface motion correctly, the correct calculations of the relevant parameters for the time domain equations (7) and (8) are very important. Among them, the calculation of the added mass at the infinite frequency is extremely important. Due to the limitation of the panels in the numerical simulation, the calculation of the added mass at infinite frequency is not reliable as other conventional hydrodynamic parameters, which may cause
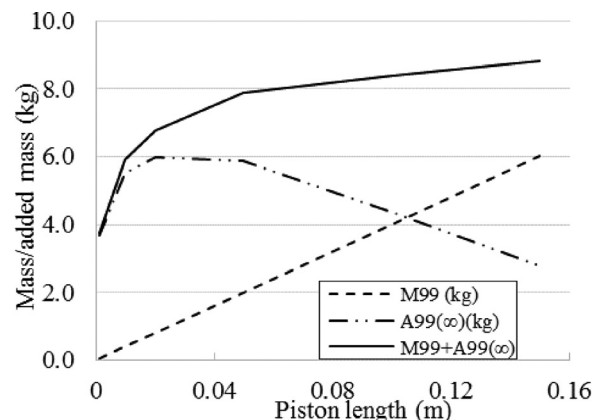

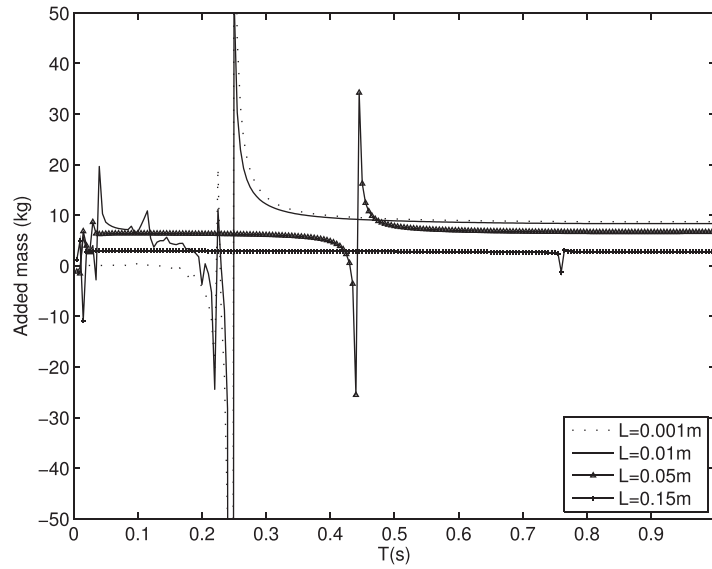FIG. 8. Masses and the added masses of the pistons in different lengths.

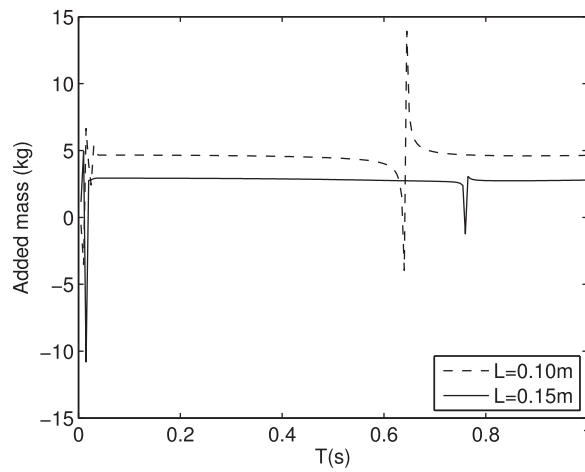FIG. 9. Added mass predictions for the pistons with different lengths.

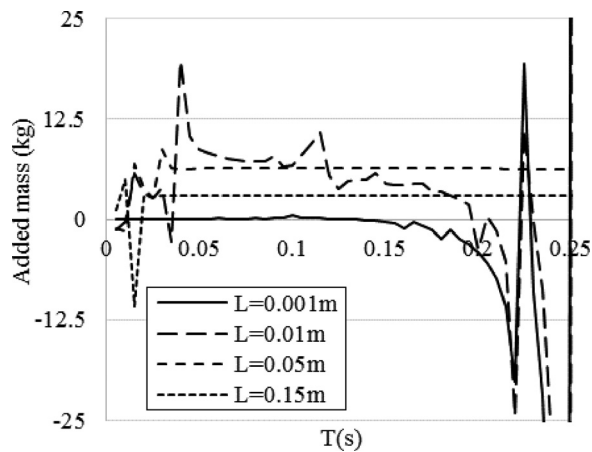FIG. 10. Added mass predictions for the pistons (L = 0.10 m and L = 0.15 m).

FIG. 11. Added mass in high frequency waves (very short waves).

serious problems in the time-domain analysis, because the dynamic responses are fully related to the overall mass in the dynamic system. This becomes more obvious when the piston is chosen as a massless (i.e., a zero-length piston) or a very thin piston, the added mass at the infinite frequency may be wrongly calculated (the huge spiky added mass for very short waves, see Figure 11). The reason for this may be due to the zero or very short length of the piston for which the corresponding natural period of the piston itself may be extremely small.

Relatively, the added mass at the infinite frequency is more reliable and may be easier to obtain when the piston is long.

The utilisation of the different pistons in the numerical simulation of the OWC wave energy converters may have some practical benefits and considerations. As it is shown that for a full-length of a piston, it seems beneficial because more reliable and stable added mass can be relatively easy to attain. However, a full length piston in an OWC device is only possible when the OWC has a uniform water column. Unfortunately, this is not the case in many engineering applications. A good example is the BBDB OWC device.[14,40,41] Their bent duct of the BBDB device does not allow a full length of a piston to be implemented if a two-body system is used. Hence, it is an advantage to choose an appropriate length of the piston for representing the internal water surface in this regard.

In some practical applications, people have to make a decision how large of the frequency is enough when its added mass can be taken as the added mass at infinite frequency. Table III shows the added mass at different frequencies for the pistons with different lengths. When the massless piston is used, the added mass at infinite frequency is a large negative value, which is obviously incorrect. For short lengths of the pistons, its added mass will be very varying regarding to the frequencies. In this particular example, when the piston length is longer than 0.05 m, the added mass tends to be steady regardless of the frequencies (also see Figure 12). However, it must be noted that even for the longest piston ($L = 0.15$ m), its added mass at very high frequency can be unsteady significantly (see Figure 11). Hence, it can be very tricky when the added mass is decided if the real added mass at infinite frequency is not available. In addition, for the case of massless piston, or the very short piston ($L < 0.05$ m), the added mass at infinite frequency is not well predicted. This may cause a large variation when the added mass at infinite frequency is calculated when compared to other cases in Table III.

D. Piston length and hydrodynamic damping coefficient

For the pistons with different lengths, the damping coefficients are all very close, especially when the wave periods are long, for instance, larger than 0.5 s (see Figures 13(a) and 13(b)), and for very short pistons, the vibrant damping coefficients can be seen in very short waves when its period is less than 0.25 s. In this vibrant coefficients, negative damping coefficients can be also seen. It is believed that the negative damping coefficients may be caused by the inappropriate panel sizes for those very short waves. If the pistons are longer, the vibrant damping coefficients are less severe. However, it can be seen that corresponding to the inherent natural periods, the damping coefficients exhibit large changes (see Figure 13(b)).

TABLE III. Added mass (in kg) at different frequencies.

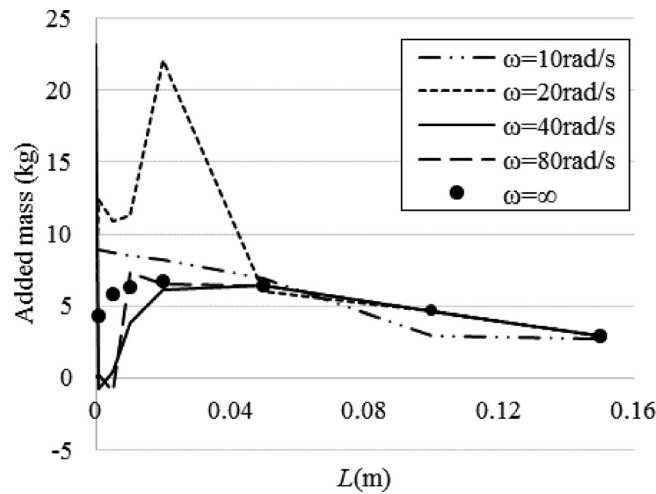| L(m)	$\omega = 10$ rad/s	$\omega = 20$ rad/s	$\omega = 40$ rad/s	$\omega = 80$ rad/s	$\omega = \infty$
0	8.869	6.833	23.177	0.043	−70.10
0.001	8.918	12.369	−0.713	0.282	4.348
0.005	8.751	10.915	0.437	−0.995	5.771
0.01	8.551	11.345	3.784	7.272	6.304
0.02	8.158	22.029	6.074	6.559	6.663
0.05	6.907	6.055	6.373	6.418	6.429
0.1	2.967	4.608	4.650	4.662	4.662
0.15	2.746	2.903	2.927	2.933	2.934

FIG. 12. Added mass at different frequencies for different "pistons" (compared to the added mass "black dots" at infinite frequency).

E. Piston length and impulse function

Figure 14 shows the comparison of the impulse functions for the heave motions of the pistons of different lengths. It can be seen that impulse functions are very similar, regardless of the piston lengths. One can notice that for the piston of length 0.10 m, some high frequency oscillations can be seen for a long time, which is corresponding to large spike at its inherent natural period. It will be seen later in the research that the small oscillations in the impulse function for $L = 0.10$ m will not cause any problem in the time-domain simulation, because this frequency of the impulse function oscillation is very different from that of the natural frequency of the dynamic system, and its influence to the motion responses is very small.

In the calculation of the impulse functions, the spiky damping coefficients must be taken carefully, otherwise it can create a very vibrant oscillation in the impulse functions. To get good impulse functions shown in Figure 14, the hydrodynamic damping coefficients are actually those shown in Figure 15, in which the very spiky damping coefficients in high frequencies should not be included in the calculation.

F. Piston length and excitation

Figure 16 shows a comparison of the excitation given in the WAMIT simulations. It can be seen that when the wave periods is longer than 1.0 s, the excitations for the different pistons
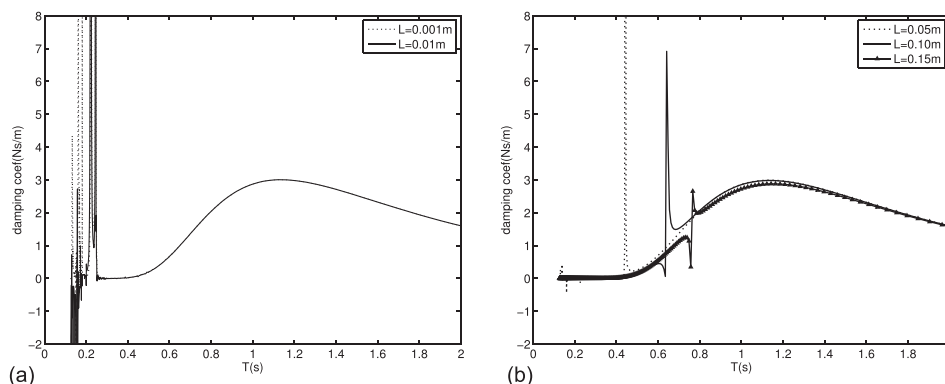

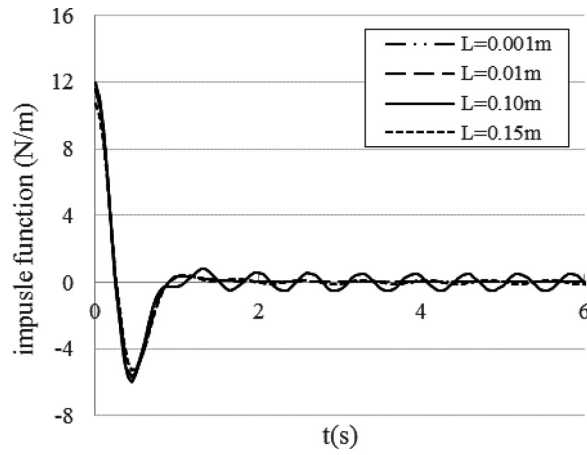FIG. 13. Damping coefficients for the pistons of different lengths.

FIG. 14. Impulse functions for the pistons of different lengths.
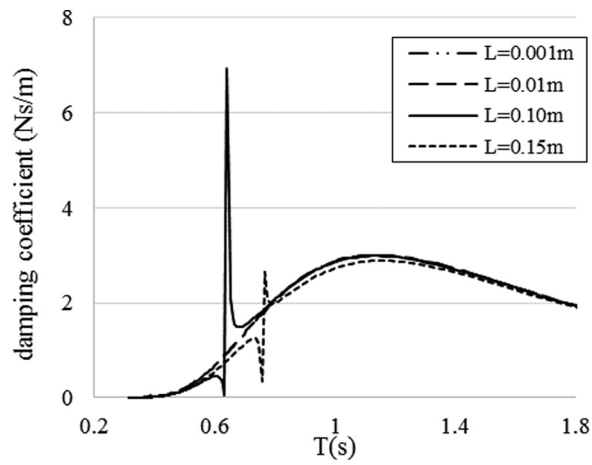

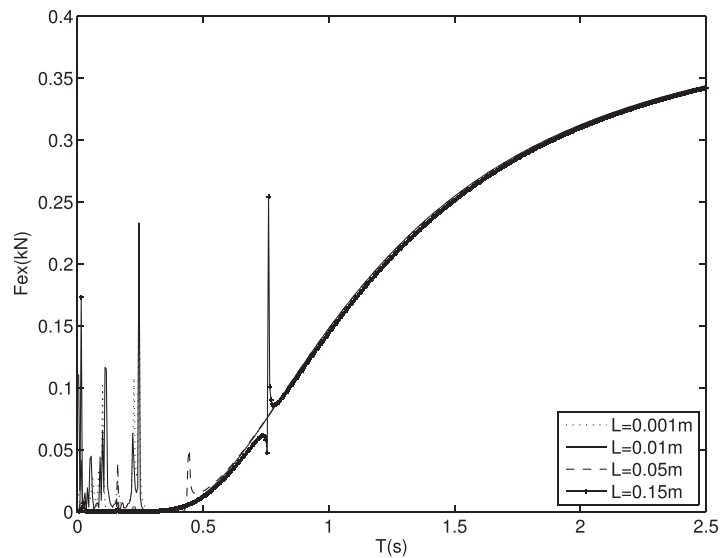FIG. 15. Damping coefficients for the piston of different lengths.

FIG. 16. Excitations on the pistons of difference lengths.

are almost identical. However, for very short wave periods, the excitation can be very spiky (see both Figures 16 and 17). The maximum values can be much larger than the excitation in the longer waves. The reason for this may be the interaction between the float and the piston, and it may be also caused due to the panel limitation for the calculation in very short waves (see the following comments on this issue). However, the very large spiky excitations do not create same spiky motion responses (see Figures 3 and 6). The reason why the very spiky excitations do not generate large responses is that the corresponding periods are much shorter than the natural periods of the pistons in the dynamic system.

1. Comments on the piston representation

Some additional comments are given as follows:

First of all, in the boundary element method employed in this study, the generation of the appropriate panels must be considered carefully. For a good simulation, as a rule of thumb, the largest length of the panels in the simulation must be smaller than 1/7 of the wave length.[42] Meanwhile, a good practice in the panel generation is to avoid any rapid change in the sizes of the adjacent panels. Ideally, the adjacent panels would have a similar size (WAMIT manual). In this regard, the simulation at the infinite frequency or very high frequencies may be not satisfactory, since the panels satisfying the conditions are impossible. However, this does not mean the calculation of the added mass at infinite frequency can not be conducted. Examples have shown that the reliable results for the added mass at infinite frequency may be obtained, but care must be taken for those very short pistons as shown in the example.

The second comment will be on the natural periods of the pistons. If there is no interaction between the piston and the device itself, a thin piston would have a short natural period in heave according to Eqs. (12), (14), or (15) (note: in the calculation, L should be taken as the actual length of the piston, rather than the length of the water column). In this regard, it can be deduced that the heave resonance period will be longer for a longer piston. Then why all the pistons mentioned above have same natural periods, regardless of the piston lengths?

Indeed, the thin piston has a short natural period in heave, which can be given by Eqs. (12), (14), or (15), and this will become evident when we look at the effect of the piston lengths later in the research. However, due to the interaction between the float body and the imaginary pistons, in the dynamic system, the mass and added mass must be considered together, as shown in Table II. Meanwhile, it can be also understood when a very thin piston is considered, it will perform as a "wave rider," which only follows the motion of the water body in the water column in waves. Hence in this regard, the motion of the water body (i.e., the full piston) decides the motion of the piston. This may explain why different pistons experience same responses.
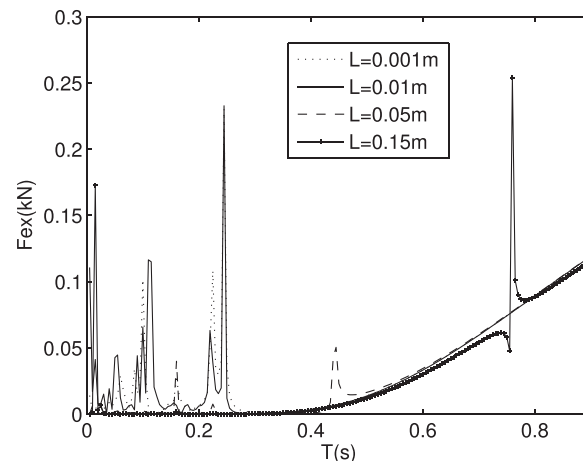

FIG. 17. Excitations on the pistons of difference lengths (zoom).

IV. RESULTS AND ANALYSIS

For studying the time domain analysis, irregular waves of a significant wave height $H_s = 0.1$ m and a mean period of $T_{01} = 1.0$ s are chosen due to its closeness to the resonance periods of the piston motion ($T_0 = 0.934$ s).

In the irregular waves, the effects of the infinite frequency added mass to the motions are examined here. An important factor in the time domain analysis is the assessment of the added mass at infinite frequency. From the time domain equations (7) and (8), the natural frequency of the dynamic system will be very much decided by the restoring coefficient and the total mass (structure or piston mass plus their added mass at infinite frequency). Hence, the reliable computation of the added mass at infinite frequency is of vital importance.

As shown in Ref. 43, the time domain result can be checked when it is compared to the transferred result from the frequency domain response, because the later analysis has only related to the parameters at the relevant wave frequencies, rather than the problems in assessing the infinite frequency added mass.

A. Criteria of accuracy

Following Sheng and Lewis,[44] two values are used to assess the goodness of the time-domain simulation. The first value is the commonly used correlation coefficient ("R"), which is a good indicator of the two time-series in phase comparison, but not in the relative amplitudes. For instance, when two time series are fully in phase regardless of their very different amplitudes, the correlation between them would be a unit.

The correlation coefficient is calculated as

$$R = \frac{\sum_{i=1}^{N}(x_i - \bar{x})(y_i - \bar{y})}{\sqrt{\sum_{i=1}^{N}(x_i - \bar{x})^2 \sum_{i=1}^{N}(y_i - \bar{y})^2}}. \tag{16}$$

The second value is the relative square root error ("RRE"), which can be used for distinguishing the actual difference between the two time series. This relative square root error is employed because it removes the effects of the absolute amplitude in the target time series. The RRE can be calculated as

$$RRE = \sqrt{\frac{\sum_{i=1}^{N}(y_i - x_i)^2}{\sqrt{\sum_{i=1}^{N}(y_i - \bar{y})^2}}}. \tag{17}$$

B. Bottom-fixed OWC

In the first case, the time domain analyses have been conducted for the OWC device in a fixed manner, hence there is no motion for the device, but the piston heave motion (i.e., the internal water surface in this case) can be calculated without a consideration of the device heave motion. Figures 18–22 show the comparisons between the time domain analysis and the frequency domain analysis for the different length pistons. It can be seen when the piston is very short, the time domain simulation shows significant differences to the result from the frequency domain analysis (see Figures 18 and 19). The main reason for the difference is the added mass at infinite frequency, as it can be seen in Figure 8, for the very short piston, the added mass at infinite frequency is well underpredicted, hence the corresponding dynamic system for a very short piston would have a higher natural frequency than it should be, so in the specific irregular
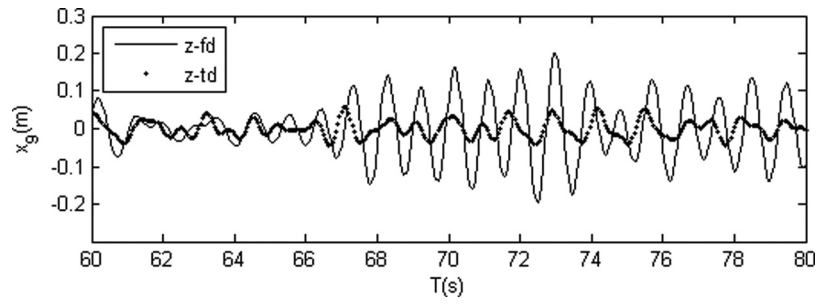
FIG. 18. Heave motion of the piston (piston length L = 0.001 m).
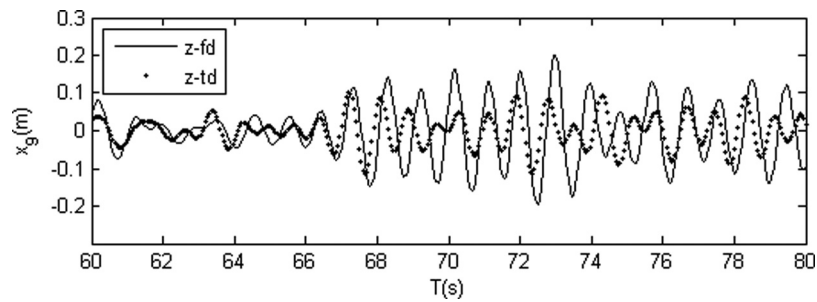
FIG. 19. Heave motion of the piston (piston length L = 0.01 m).
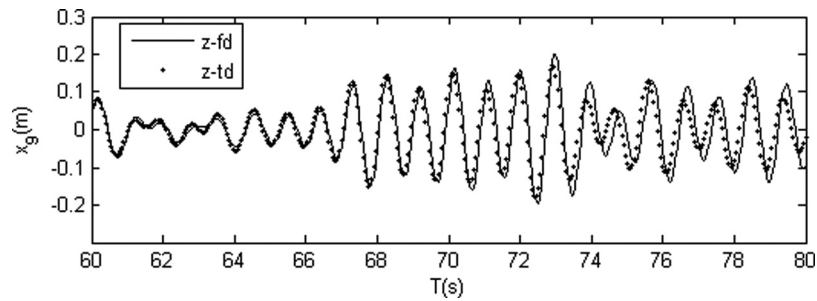
FIG. 20. Heave motion of the piston (piston length L = 0.05 m).
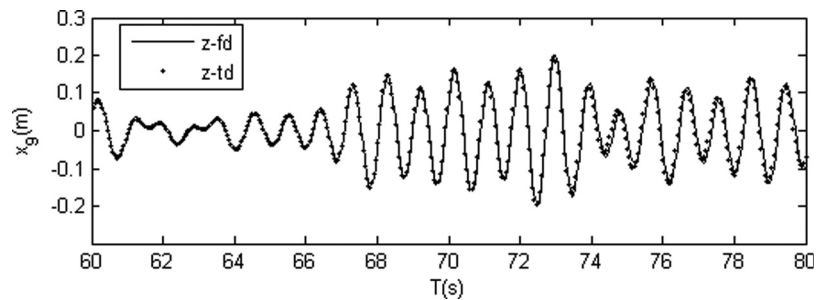
FIG. 21. Heave motion of the piston (piston length L = 0.10 m).
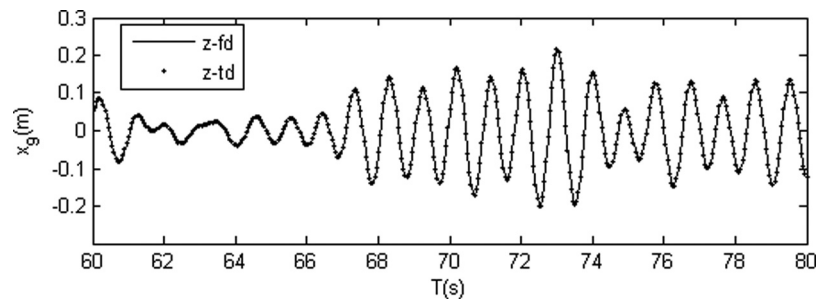
FIG. 22. Heave motion of the piston (piston length L = 0.15 m).

wave, the heave motion of the piston is far away from the resonance with the wave, that is why the amplitude of the piston heave motion is much smaller than it should be (note: the damping and the excitation for all pistons are very similar from Figures 16 and 14).

When the piston is getting longer, better time domain result can be seen, because their calculated overall mass is getting closer to the actual one, and thus the dynamic system would have a closer natural frequency to the actual one. For the lengths $L = 0.10$ m and $L = 0.15$ m, the time-domain result is almost identical to that from the frequency domain (Figures 21 and 22). Table IV shows the accuracy of the time domain analysis. It can be seen that in the cases of the very short pistons, the accuracy of the time domain analysis is very low. The correlation coefficient is getting larger when the piston is getting longer, while the RRE is getting smaller, which indicates the closeness of the two time series. For the cases of $L = 0.10$ m and $L = 0.15$ m, the correlation coefficients are close to unit, which means that the two time series are very much in phase, while the corresponding small RRE means a small difference between the two time series.

C. Floating OWC

Similar to the cases of the bottom-fixed OWC, the time domain analyses have been carried out for the floating OWC device, in which the OWC device itself and the imaginary piston can both move un-restrainedly. Figures 23–26 show the comparisons between the time domain and the frequency domain analyses when the pistons of different lengths are used. Again, it can be seen that when the piston is very short, the time domain simulation shows significant difference to that from the frequency domain analysis (see Figure 23). When the piston is getting longer, better time domain analysis result can be seen. Again, for the lengths $L = 0.10$ m and $L = 0.15$ m, the time-domain result is same as that from the frequency domain (Figures 25 and 26). Table V shows the accuracy analysis of the time domain simulations, which is very similar to Table IV, and hence same conclusions can also be drawn.

It must be pointed out that the prediction of the heave motion of structure is better reproduced than that of the heave motion of piston, especially when the piston is short. The reason for this is the added mass at infinite frequency for the device heave motion is very much reliable regardless of the piston lengths (see Table II). However, it must be also noted that the heave motions of the two bodies are coupled together (from Eqs. (7) and (8)), the inaccurate prediction of the piston heave motion would have eventually affected the heave motion of the device. That is why we can see some differences of the heave motion between the time domain

TABLE IV. Accuracy analysis of the time domain simulations.

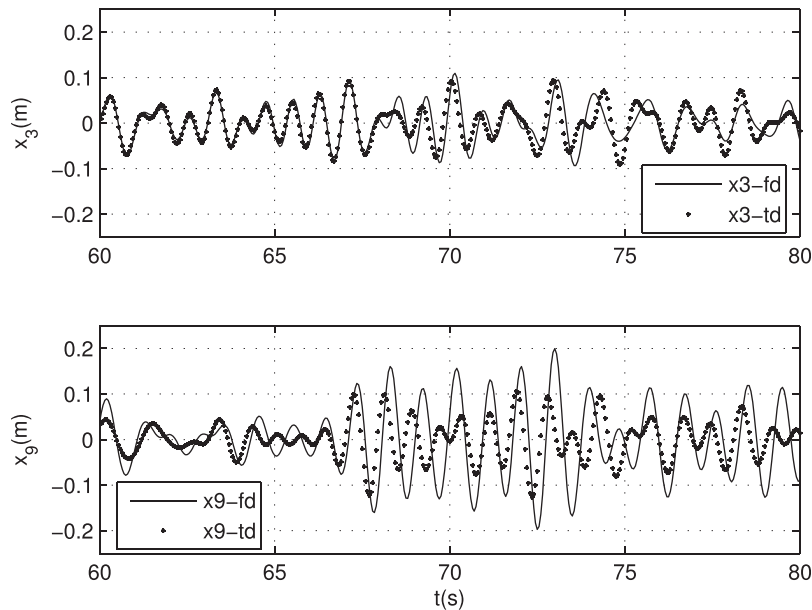|	$L = 0.001$ m	$L = 0.01$ m	$L = 0.05$ m	$L = 0.10$ m	$L = 0.15$ m
R	0.395	0.328	0.870	0.974	0.999
RRE	0.925	0.967	0.494	0.226	0.047

FIG. 23. Heave motions of the floating structure and the piston (piston length L = 0.01 m).

and the frequency domain analyses for the very short piston (see Figure 23), though the corresponding added mass at the infinite frequency is well calculated (also see Table II).

V. CONCLUSIONS

In hydrodynamic study of OWC wave energy converters, different methods have been developed in frequency domain if a linear dynamic system is assumed. However, for a full scale OWC or the practical OWC plant, its dynamics may be nonlinear due to the factors of the nonlinear air compressibility and maybe of a nonlinear air turbine (PTO). Hence, for such a dynamic system, time-domain analysis must be conducted. In this research, we focus on a two-
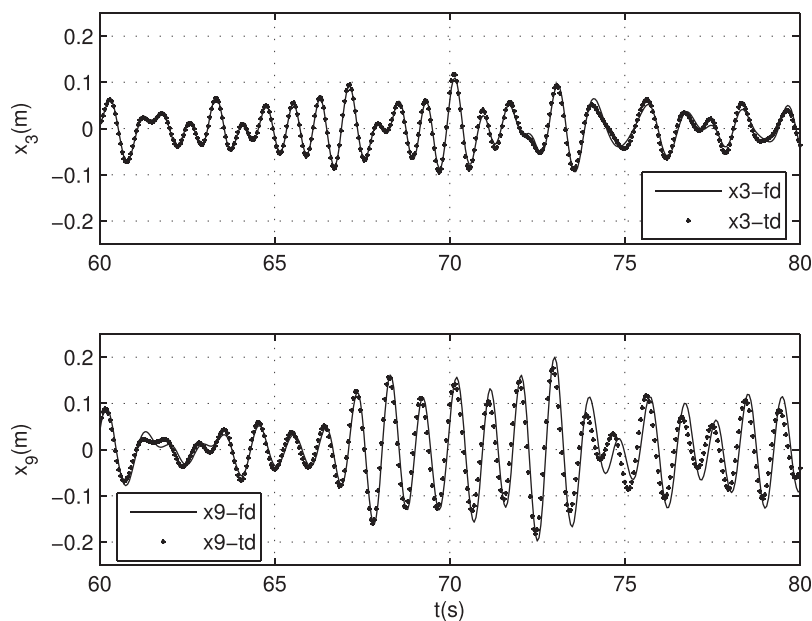

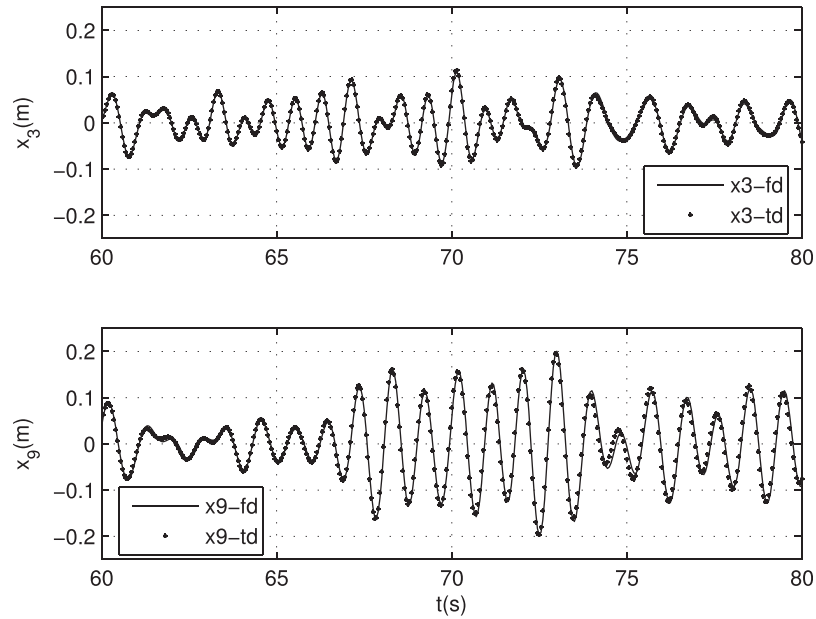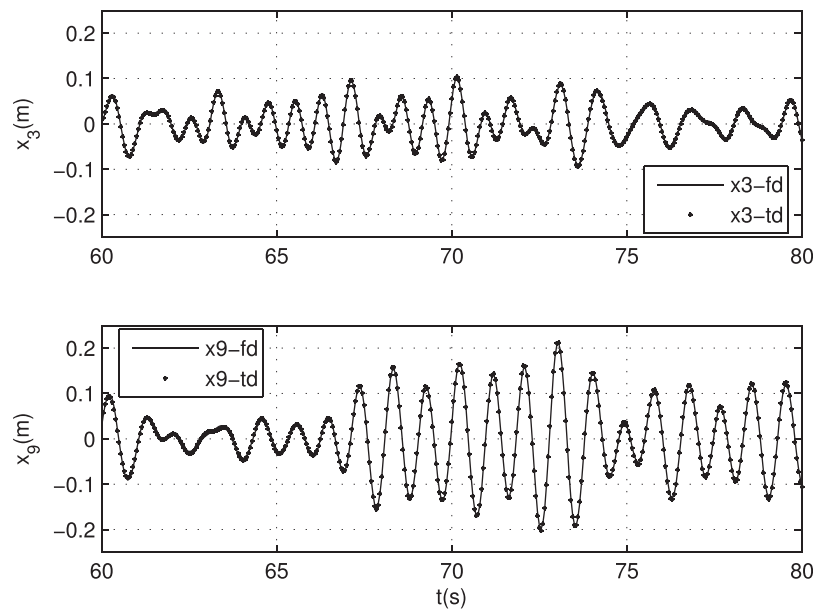FIG. 24. Heave motions of the floating structure and the piston (piston length L = 0.05 m).

FIG. 25. Heave motions of the floating structure and the piston (piston length L = 0.10 m).

FIG. 26. Heave motions of the floating structure and the piston (piston length L = 0.15 m).

TABLE V. Accuracy analysis of the time domain simulations.

	$L = 0.001$ m	$L = 0.01$ m	$L = 0.05$ m	$L = 0.10$ m	$L = 0.15$ m
R	0.423	0.401	0.908	0.981	0.999
RRE	0.914	0.929	0.419	0.194	0.060

body system to represent the device itself and the imaginary piston for the OWC wave energy converter for their hydrodynamics. The main reason for such a consideration is that the two-body system has a very clear physical meaning and the study and implementation of the two-body system are very straightforward.

In implementing the time-domain analysis, the Cummins-Ogilvie's equation is used, in which the hydrodynamic parameters are transformed from the parameters in the frequency-domain analysis to time domain, such as the added mass at infinite frequency and the impulse functions. In the research work, we examine how reliable we can conduct a time domain analysis for the hydrodynamic performance of an OWC wave energy converter.

From the results and the analyses, following conclusions can be drawn:

(i)   The length of the imaginary piston for the water body in the water column has little influence on the responses of the motions for the frequency range of interest.

(ii)   In very short waves (high frequency waves), there will be vibrant responses in added mass, damping coefficients, and the excitation, though these spiky responses have no significant effect on the overall responses of motions in frequency domain analysis, but they tend to cause problems when we choose the added mass at infinite frequency or at a very large frequency, or the calculation of the impulse function. As a result of these difficulties, the time domain solution based on these parameters may not be appropriate.

(iii)   The examples show that a favourable length of the piston must be chosen so that reliable time-domain analysis can be obtained.

[1]A. Falcao, "Wave energy utilization: A review of the technologies," Renewable Sustainable Energy Rev. **14**, 899–918 (2010).

[2]J. F. Chozas, "Technical and non-technical issues towards the commercialisation of wave energy converters," Ph.D. thesis (Department of Civil Engineering, Aarborg University, Aarborg, Denmark, 2013).

[3]T. Heath, "A review of oscillating water columns," Philos. Trans. R. Soc. London, Ser. A **370**, 235–245 (2012).

[4]Y. Torre-Enciso, I. Ortubia, L. I. Lopez de Aguileta, and J. Marques, "Mutriku wave power plant: From the thinking out to the reality," in Proceedings of the 8th European Wave and Tidal Energy Conference, Uppsala, Sweden, 7–10 September 2009.

[5]D. L. O'Sullivan and A. W. Lewis, "Generator selection and comparative performance in offshore oscillating water column ocean wave energy converters," IEEE Trans. Energy Convers. **26**, 603–614 (2011).

[6]A. J. N. A. Sarmento and A. F. D. O. Falcao, "Wave generation by an oscillating surface pressure and its application in wave-energy extraction," J. Fluid Mech. **150**, 467–485 (1985).

[7]D. V. Evans, "Wave-power absorption by systems of oscillating surface pressure distributions," J. Fluid Mech. **114**, 481–499 (1982).

[8]D. V. Evans and R. Porter, "Hydrodynamic characteristics of an oscillating water column device," Appl. Ocean Res. **17**, 155–164 (1995).

[9]J. Weber, "Representation of non-linear aero-thermodynamics effects during small scale physical modelling of OWC WECs," in Proceedings of the 7th European Wave and Tidal Energy Conference, Porto, Portugal, 11–14 September 2007.

[10]W. Sheng, R. Alcorn, and A. Lewis, "Physical modelling of wave energy converters," Ocean Eng. **84**, 29–36 (2014).

[11]A. J. N. A. Sarmento, L. M. C. Gato, and A. F. de O. Falcao, "Turbine-controlled wave energy absorption by oscillating water column devices," Ocean Eng. **17**, 481–497 (1990).

[12]W. Sheng, R. Alcorn, and A. Lewis, "On thermodynamics of primary energy conversion of OWC wave energy converters," J. Renewable Sustainable Energy **5**, 023105 (2013).

[13]W. Sheng, R. Alcorn, and A. Lewis, "Primary wave energy conversions of oscillating water columns," in Proceedings of the EWTEC 2013 Conference, Aalborg, Denmark, 2–5 September 2013.

[14]K. Toyota, S. Nagata, Y. Imai, J. Oda, and T. Setoguchi, "Primary energy conversion characteristics of a floating OWC "Backward Bent Duct Buoy"," in Proceedings of 20th International Offshore and Polar Engineering Conference, Beijing, China, 20–25 June 2010.

[15]Y. Imai, K. Toyota, S. Nagata, T. Setoguchi, and M. Takao, "An experimental study on generating efficiency of a wave energy converter "Backward Bent Duct Buoy"," in Proceedings of the 9th European Wave and Tidal Energy Conference, Southampton, UK, 5–9 September 2011.

[16]M. T. Morris-Thomas, R. J. Irvin, and K. P. Thiagarajan, "An investigation into the hydrodynamic efficiency of an oscillating water column," J. Offshore Mech. Arct. Eng. **129**, 273–278 (2007).

[17]H. Martins-rivas and C.-C. Mei, "Wave power extraction from an oscillating water column along a straight coast," Ocean Eng. **36**, 426–433 (2009).

[18]S. A. Mavrakos and D. N. Konispoliatis, "Hydrodynamic analysis of a vertical axisymmetric oscillating water column device floating in finite depth waters," in Proceedings of the ASME 31st International Conference on Ocean, Offshore and Arctic Engineering, Rio de Janeiro, Brazil, 1–6 July 2012.

[19]C. H. Lee and F. G. Nielsen, "Analysis of oscillating-water-column device using a panel method," in International Workshop on Water Wave and Floating Bodies, Hamburg, Germany, 17–20 March 1996.

[20]O. M. Faltinsen, O. F. Rognebakke, and A. N. Timokha, "Two-dimensional resonant piston-like sloshing in a moonpool," J. Fluid Mech. **575**, 359–397 (2007).

[21]C. Maisondieu and P. Ferrant, "Evaluation of the 3D flow dynamics in a moonpool," in Proceedings of the Thirteenth International Offshore and Polar Engineering Conference, Honolulu, Hawaii, USA, 25–30 May 2003.

[22]P. McIver, "Resonances of a heaving structure with a moonpool," in Proceedings of IWWWFB19, Cortona, Italy, 28–31 March 2004.

[23]R. v. Veer and H. J. Thorlen, "Added resistance of moonpool in calm water," in Proceedings of the ASME 27th International Conference on Offshore Mechanics and Arctic Engineering, Estoril, Portugal, 15–20 June 2008.

[24]D. V. Evans, "The oscillating water column wave-energy device," IMA J. Appl. Math. **22**, 423–433 (1978).

[25]A. Falcao, J. C. C. Henriques, and J. J. Candido, "Dynamic and optimization of the OWC spar buoy wave energy converter," Renewable Energy **48**, 369–381 (2012).

[26]J. C. C. Henriques, A. Falcao, R. P. F. Gomes, and L. M. C. Gato, "Air turbine and primary converter matching in spar-buoy oscillating water column wave energy device," in Proceedings of the 32nd International Conference on Ocean, Offshore and Arctic Engineering, Nantes, France, 9–14 June 2013.

[27]A. Babarit, J. Hals, M. J. Muliawan, A. Kurniawan, T. Moan, and J. Krogstad, "Numerical benchmarking study of a selection of wave energy converters," Renewable Energy **41**, 44–63 (2012).

[28]A. Kurniawan, J. Hals, and T. Moan, Modelling and simulation of a floating oscillating water column, Proceedings of the ASME 2011 30th International Conference on Ocean, Offshore and Arctic Engineering, Rotterdam, The Netherlands, 19–24 June 2011.

[29]J. Falnes, *Ocean Waves and Oscillating Systems: Linear Interaction Including Wave-Energy Extraction* (Cambridge University Press, 2002).

[30]A. F. d. O. Falcao and P. A. P. Justino, "OWC wave energy devices with air flow control," Ocean Eng. **26**, 1275–1295 (1999).

[31]W. E. Cummins, The impulse response function and ship motions, Report No. 1661, Department of the Navy, David Taylor Model Basin, USA, 1962.

[32]T. F. Ogilvie, "Recent progress toward the understanding and prediction of ship motions," in Proceedings of the 5th Symposium on Naval Hydrodynamics, Washington DC, USA, 1964.

[33]M. Alves, M. Vicente, A. Sarmento, and M. Guerinel, "Implementation and validation of a time domain model to simulate the dynamics of OWCs," in Proceedings of the 9th European Wave and Tidal Energy Conference, Southampton, UK, 5–9 September 2011.

[34]A. Falcao, J. J. Candido, P. A. P. Justino, and J. C. C. Henriques, "Hydrodynamics of the IPS buoy wave energy converter including the effect of non-uniform acceleration tube cross section," Renewable Energy **41**, 105–114 (2012).

[35]F. Kara, "Time domain prediction of power absorption from ocean waves with latching control," Renewable Energy **35**, 423–434 (2010).

[36]R. Taghipour, T. Perez, and T. Moan, "Hybrid frequency-time domain models for dynamic response analysis of marine structures," Ocean Eng. **35**, 685–705 (2008).

[37]W. Sheng, R. Alcorn, and A. Lewis, "Numerical assessment on primary wave energy conversion of oscillating water columns (OMAE2014-23218)," in Proceedings of the ASME 2014 33rd International Conference on Ocean, Offshore and Arctic Engineering, San Francisco, USA, 8–13 June 2014.

[38]M. E. McCormick, *Ocean Wave Energy Conversion* (Dover Publications, Inc., 2007).

[39]C. H. Lee, J. N. Newman, and F. G. Nielsen, "Wave interaction with an oscillating water column," in Proceedings of the 6th International Offshore and Polar Engineering Conference (ISOPE'96), Los Angeles, USA, 26–31 May 1996.

[40]D. C. Hong, S. Y. Hong, and S. W. Hong, "Numerical study on the reverse drift force of floating BBDB wave energy absorbers," Ocean Eng. **31**, 1257–1294 (2004).

[41]K. Toyota, S. Nagata, Y. Imai, and T. Setoguchi, "Effects of hull shape on primary conversion characteristics of a floating OWC "Backward Bent Duct Buoy"," J. Fluid Sci. Technol. **3**, 458–465 (2008).

[42]O. M. Faltinsen, *Sea loads on Ships and Offshore Structures* (Cambridge University Press, 1990).

[43]W. Sheng and A. Lewis, "Assessment of wave energy extraction from seas: numerical validation," J. Energy Resour. Technol. **134**, 041701 (2012).

[44]W. Sheng and A. Lewis, "Short-term prediction of an artificial neural network in an oscillating water column," Inter. J. Offshore Polar Eng. **21**, 248–255 (2011).